Accepted version

Journal Pre-proof

Effect of Hudson Bay closure on global and regional climate under different astronomical configurations

Zhipeng Wu, Qiuzhen Yin, Andrey Ganopolski, André Berger, Zhengtang Guo

PII: S0921-8181(23)00013-9

DOI: https://doi.org/10.1016/j.gloplacha.2023.104040

Reference: GLOBAL 104040

To appear in: *Global and Planetary Change*

Received date: 1 November 2022

Revised date: 7 January 2023

Accepted date: 11 January 2023

Please cite this article as: Z. Wu, Q. Yin, A. Ganopolski, et al., Effect of Hudson Bay closure on global and regional climate under different astronomical configurations, *Global and Planetary Change* (2023), https://doi.org/10.1016/j.gloplacha.2023.104040

This is a PDF file of an article that has undergone enhancements after acceptance, such as the addition of a cover page and metadata, and formatting for readability, but it is not yet the definitive version of record. This version will undergo additional copyediting, typesetting and review before it is published in its final form, but we are providing this version to give early visibility of the article. Please note that, during the production process, errors may be discovered which could affect the content, and all legal disclaimers that apply to the journal pertain.

© 2023 Published by Elsevier B.V.

Journal Pre-proof

Effect of Hudson Bay closure on global and regional climate under different astronomical configurations

Zhipeng Wu[a,b,c*], Qiuzhen Yin[a*], Andrey Ganopolski[d], André Berger[a], Zhengtang Guo[b,c,e]

[a]Georges Lemaître Center for Earth and Climate Research, Earth and Life Institute, Université catholique de Louvain, Louvain-la-Neuve, Belgium

[b]Key Laboratory of Cenozoic Geology and Environment, Institute of Geology and Geophysics, Chinese Academy of Sciences, Beijing, China

[c]University of Chinese Academy of Sciences, Beijing, China

[d]Potsdam Institute for Climate Impact Research, Potsdam, Germany

[e]CAS Center for Excellence in Life and Paleoenvironment, Beijing, China

*Corresponding authors

E-mail address: zhipeng.wu@uclouvain.be (Z.P. Wu); qiuzhen.yin@uclouvain.be (Q.Z. Yin)

Address: Université catholique de Louvain, Place Louis Pasteur, 3, L4.03.08, B-1348, Louvain-la-Neuve, Belgium.

Abstract: During the Quaternary, the Hudson Bay switched between closed (covered by ice sheet) and open (ice sheet-free) condition due to large variations of ice sheets. However, how the closure and opening of the Hudson Bay have affected the local and global climates is still poorly understood. Using the LOVECLIM1.3 model, here we investigate the effect of the Hudson Bay closure under glacial conditions with different astronomical configurations, greenhouse gases (GHG) concentrations and Northern Hemisphere (NH) ice volume. Our model results show that the closure of the Hudson Bay could lead to a strengthening of the Atlantic Meridional Overturning Circulation (AMOC), which in turn leads to a warming in the Northern Hemisphere with notable warming in the Labrador Sea and northeast North Atlantic, a cooling in the Southern Hemisphere and a northward shift of the Inter-tropical Convergence Zone (ITCZ). In addition to the large-scale climate changes, the closure of Hudson Bay also leads to a

Journal Pre-proof

strong cooling over the Hudson Bay region due to changes of surface properties and a cooling to the southeast of Greenland due to more wind-driven sea ice export from the Arctic. However, the effect of the Hudson Bay closure depends on background climate conditions, and it could weaken or slightly reinforce the effect of the ice sheets for different astronomical configurations.

Keywords: Hudson Bay, AMOC, ice sheets, glacial simulations, astronomical forcing

1. Introduction

The Hudson Bay is one of the largest inland seas in the world and it receives a large amount of freshwater through riverine input (~760 km^3/yr; Déry et al., 2011). It is connected with the Arctic Ocean through the Canadian Arctic Archipelago and with the Labrador Sea through the Hudson Strait. The outflow through Hudson Strait into the Labrador Sea and on to the North Atlantic is thought to play an important role in the Labrador current, the northern North Atlantic circulation and its dense water formation (Fig. 1; Straneo and Saucier, 2008). It thus has a great effect on the weather/climate of the Northern Hemisphere (NH), especially in the Labrador Sea and Atlantic, and perhaps over the whole globe (dos Santos et al., 2010).

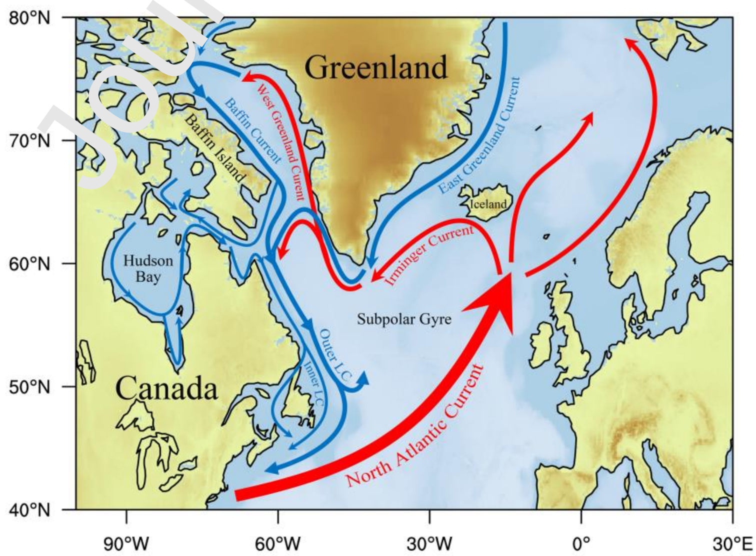

Fig. 1 Map of Hudson Bay and surroundings showing modern surface circulations with cold (blue) and warm (red) currents (adopted from Straneo and Saucier, 2008; Lochte

Journal Pre-proof

et al., 2020). The topography data is from https://www.ngdc.noaa.gov.

Due to the importance of the Hudson Bay on local and remote climate, some studies have been performed on the role of the Hudson Bay on climate variations in different time periods of the past. For instance, both geological records (e.g. Lochte et al., 2019) and numerical simulations (e.g. Wagner et al., 2013) suggested that the Hudson Bay Ice Saddle collapse may have played a significant role in the noticeable reduction of the Atlantic Meridional Overturning Circulation (AMOC) and the rapid NH cooling 8200 years before present (BP). Rennermalm et al. (2007) used the University of Victoria Earth system climate model (UVic ESCM) to investigate the sensitivity of the AMOC to the variations of freshwater flux into the Arctic Ocean and the Hudson Bay through riverine input, and their results show that, compared to the Arctic Ocean, decreasing freshwater flux into the Hudson Bay has a much greater effect on intensifying the AMOC. Using an early version of LOVECLIM, Friedrich et al. (2010) found that the atmospheric anomalies over the Hudson Bay could drive freshwater release from the Hudson Bay into the Labrador Sea, which played a significant role in the centennial-to-millennial scale AMOC variability. They found that the atmospheric anomalies over the Hudson Bay were triggered by the internal variability that was caused by the stochastic excitations of the density-driven overturning circulation in the Nordic Seas. Their study also showed that the centennial-to-millennial scale AMOC variability could only happen when the Hudson Bay was open, and it was suppressed under the last glacial maximum (LGM) boundary conditions when the Hudson Bay was closed. However, sensitivity experiments taking into account the time-varying insolation, greenhouse gases concentrations (GHG) and the NH ice sheets during the last interglacial showed that the Hudson Bay closure could not prevent the abrupt reduction of AMOC which was instead strongly dependent on the external forcings (Loutre et al., 2014).

During periods of maximum extent of the Laurentide ice sheet, the Hudson Bay was the geographic center of the Laurentide ice sheet and it was covered by ice sheet during a large portion of the Quaternary. During these times, Hudson Bay was partially or completely closed, leading to a very different hydrological condition in northeastern Canada. This could cause significant changes not only in local climate but also in climate of other places through its effect on the Atlantic Ocean circulations. However, the effect of the Hudson Bay closure is seldomly investigated in paleoclimate simulations, most probably due to the technical difficulty in modifying the land-sea mask in many models, and only a few studies have taken into account the changes of the Hudson Bay during different time periods (e.g. Friedrich et al., 2010; Meccia and Mikolajewicz, 2018; Tan et al., 2020). In most transient simulations with time-dependent ice sheets covering the glacial-interglacial cycle(s), the Hudson Bay was kept open (e.g. Smith and Gregory, 2012). It is unclear how the Hudson Bay condition (open or closed) affects the regional and global climate, especially under different background climate conditions. It could be one of the factors contributing to the simulation uncertainty and to model-proxy discrepancy.

In this study, we aim to investigate the effect of the Hudson Bay closure on the mean climate state under different background conditions (different astronomical configurations, GHG concentrations and ice sheet configurations). This would help us better understand the importance of the proper treatment of the ice mask and elevation of the Laurentide ice sheet in modelling studies, especially during the glacial times. Our study is based on nine pairs of sensitivity experiments using the model LOVECLIM1.3.

Journal Pre-proof

2. Model and experiments design

LOVECLIM1.3 is a three-dimension Earth system Model of Intermediate Complexity. Detailed description of a previous version of LOVECLIM1.2 can be found in Goosse et al. (2010), and a description of LOVECLIM1.3 in Loutre et al. (2014). The model setup is the same as the one used in Yin et al. (2021). The atmosphere (ECBilt), the ocean and sea ice (CLIO) and the terrestrial biosphere (VECODE) are interactively coupled. ECBilt is a spectral atmospheric model with truncature T21, which corresponds approximately to a horizontal resolution of 5.625°×5.625°. It has three vertical layers and its dynamics are governed by the quasi-geostrophic potential vorticity. VECODE is a two-dimensional dynamical terrestrial vegetation model including two plant functional types: tree and grass, and its resolution is the same as ECBilt. CLIO is a global free-surface ocean general circulation model coupled to a thermodynamic-dynamic sea ice model. The horizontal resolution of CLIO is 3° in longitude and latitude, and there are 20 unevenly spaced levels along vertical in the ocean. LOVECLIM1.3 and its previous versions have been used in numerous studies for past, present and future climate, and the results showed that LOVECLIM can reproduce the major characteristics of climate variations both for present-day conditions and for some other important past periods (see references in Goosse et al., 2010). With respect to ocean circulations pertinent to this study, the maximum overturning streamfunction in the North Atlantic and Southern Ocean simulated by LOVECLIM show relatively good agreement with observations and proxy records, as well as with results of other models (e.g. Goosse et al., 2010; Loutre et al., 2014; Yin, 2013; Yin et al., 2021).

In this study, we performed nine pairs of experiments at nine selected dates at the beginning of each deglaciation period of the last 800 ka (Fig. 2 and Table 1). These dates were actually the initial dates for the transient interglacial climate simulations used in Yin et al. (2021) though changes of ice sheets and Hudson Bay were not considered there. At these dates, the North American ice sheet was sufficiently large to cover completely the Hudson Bay, and there are large variations in the astronomical parameters, GHG concentrations and NH ice volume. For example, obliquity ranges from 24.2º at 538 ka BP to 22.7º at 719 ka BP, precession ranges from 0.00409 at 794 ka BP to -0.00735 at 247 ka BP (Berger and Loutre, 1991), and the CO_2 equivalent (CO_{2eq}, which is calculated based on the formula in https://gml.noaa.gov/aggi/aggi.html) ranges from 267 ppmv at 424 ka BP to 171 ppmv at 719 ka BP (Luthi et al., 2008; Loulergue et al., 2008; Schilt et al., 2010). In addition, the total NH ice volume ranges from 39 million km^3 at 17 ka BP to 21 million km^3 at 424 ka BP (Ganopolski and Calov, 2011). Therefore, these experiments allow to explore the effect of the Hudson Bay closure on AMOC and the global and regional climate under different background climate conditions.

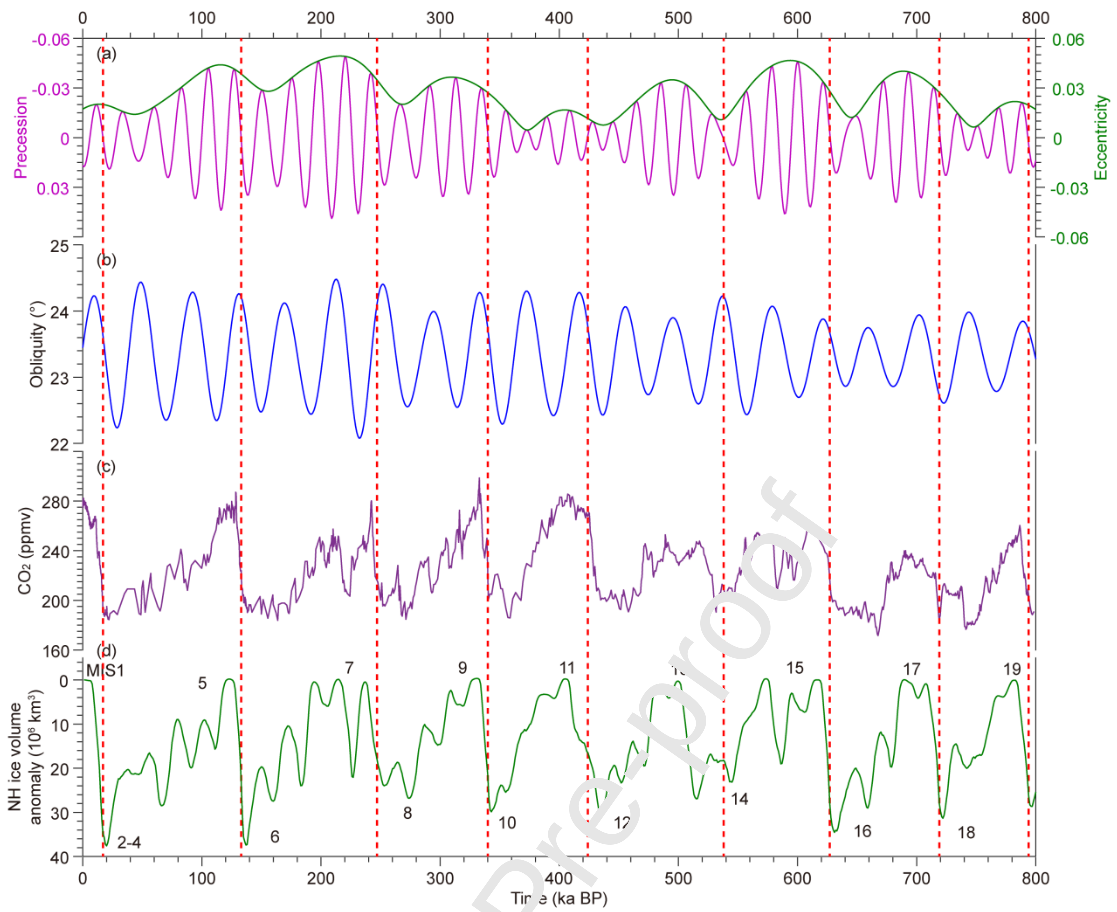

Fig. 2 Astronomical parameters (Berger and Loutre, 1991), CO_2 concentration (Luthi et al., 2008) and simulated NH ice volume anomaly as compared to the pre-industrial one (Ganopolski & Calov, 2011) of the past 800 ka. The numbers of MIS stages are indicated; the red vertical dashed lines indicate the nine selected dates.

Table 1. Astronomical parameters (Berger & Loutre, 1991), GHG concentrations (Luthi et al., 2008; Loulergue et al., 2008; Schilt et al., 2010), NH ice volume (Ganopolski & Calov, 2011) and the Hudson Bay status used in the 18 sensitivity experiments.

Experiments	Dates (ka BP)	Astronomical parameters			GHG concentrations			CO_{2eq}	NH ice volume	Hudson Bay
		Eccentricity	Obliquity (°)	Longitude of perihelion (°)	CO_2 (ppmv)	CH_4 (ppbv)	N_2O (ppbv)	(ppmv)	(million km^3)	status
17_OHB	17	0.020012	23.627	179.38	195	392	234	180	39	open

Journal Pre-proof

17_CHB											closed
133_OHB	133	0.038488	24.214	179.08	224	456	229	208	27		open
133_CHB											closed
247_OHB	247	0.034853	24.103	192.17	216	530	252	207	22		open
247_CHB											closed
340_OHB	340	0.027233	23.735	184.45	220	452	221	204	26		open
340_CHB											closed
424_OHB	424	0.011561	23.762	354.16	268	612	293	267	21		open
424_CHB											closed
538_OHB	538	0.011226	24.22	174.5	210	460	261	200	22		open
538_CHB											closed
627_OHB	627	0.028098	23.675	1[illegible].71	218	393	234	201	32		open
627_CHB											closed
719_OHB	719	0.02735	22.723	192.47	185	397	230	171	32		open
719_CHB											closed
794_OHB	794	0.01955	23.708	167.92	204	438	239	191	30		open
794_CHB											closed

At each date (and each pair), the astronomical parameters (Berger and Loutre, 1991), GHG concentrations (Luthi et al., 2008; Loulergue et al., 2008; Schilt et al., 2010) and the NH ice sheet configurations (Ganopolski and Calov, 2011) are taken at the values of this date for both experiments in each pair, the Antarctic ice sheet being kept the same as the pre-industrial one. In the presence of land ice, albedo, topography, vegetation and surface soil types corresponding to ice-covered condition (no vegetation nor soil) were prescribed at corresponding model grids in LOVECLIM1.3. Fig. 3 gives

Journal Pre-proof

an example of the NH topography anomaly at 133 ka BP and 424 ka BP relative to the pre-industrial conditions in the OHB and CHB experiments. The ice sheet data is from the simulated results of Ganopolski and Calov (2011) and interpolated to LOVECLIM grid. In addition, due to the large extent of North American ice sheet, the prescribed river routes were disrupted. For the changes of the river routes over North America, we follow the protocol for Last Glacial Maximum (LGM) experiments in the Paleoclimate Modelling Intercomparison Project-Phase 4 (PMIP4) (Kageyama et al., 2017). For instance, the river runoff that previously entered into the Hudson Bay was consequently rerouted, partly northward entering into the Arctic Ocean and partly southward entering into the Atlantic in both experiments in each pair.

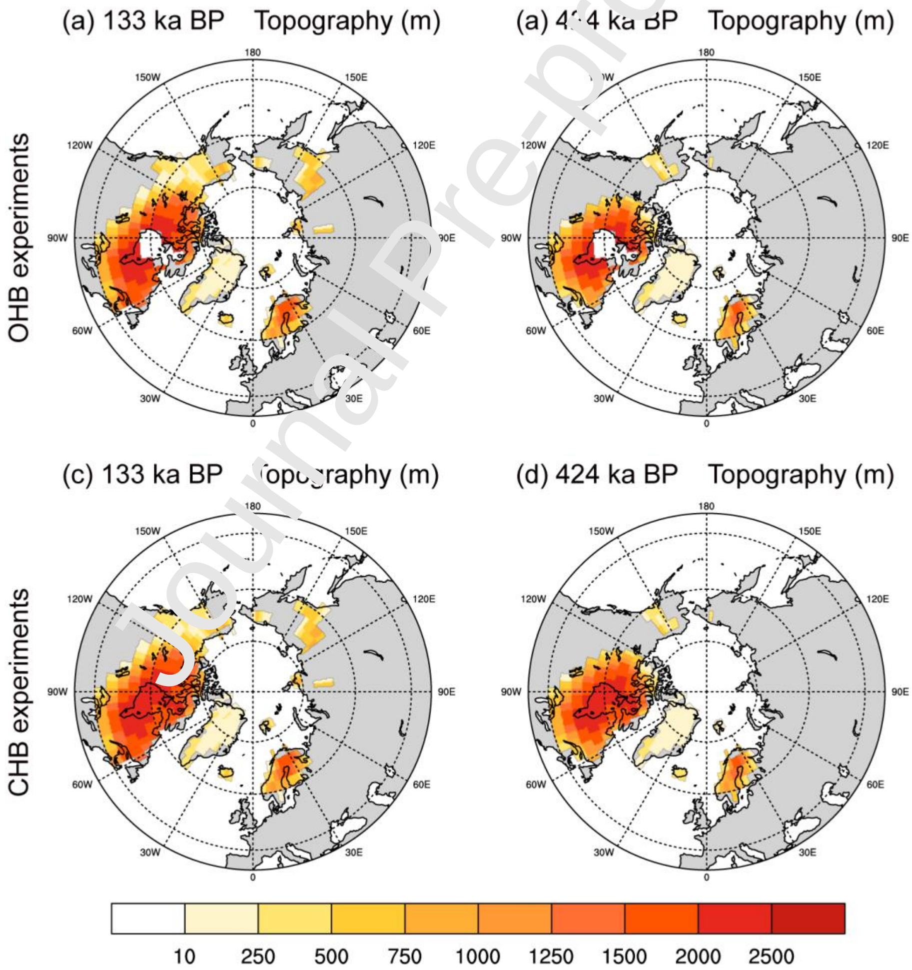

Fig. 3 Topography anomaly (m) at 133 ka BP and 424 ka BP relative to the pre-industrial conditions in the OHB and CHB experiments. The ice sheet data is from the simulated results of Ganopolski and Calov (2011) and interpolated to LOVECLIM grid.

Journal Pre-proof

Within each pair of experiments, the Hudson Bay is open in one experiment and is closed in another one (hereafter they are referred as OHB and CHB respectively). In the OHB experiments, the ocean-land mask was kept the same as the present-day one (Fig. 4a), while the ocean over the Hudson Bay was changed to land in the CHB experiments (Fig. 4b). As land ice covers only land grids in LOVECLIM1.3, the Hudson Bay was covered by land ice in the CHB experiments, while it was still kept as ocean in the OHB experiments.

All the 18 experiments were run for 2000 years to reach equilibrium, and the last 100-year average climatology was analyzed. In addition, in order to compare the effect of the Hudson Bay closure with the effect of the NH ice sheets, the snapshot experiments with the present-day ice sheets but the insolation and GHG at 133 ka BP and 424 ka BP (hereafter they are referred as OG experiments) performed by Yin et al. (2021), are also used in this study. The difference between the CHB and OHB experiments gives the impact of the Hudson Bay closure, and the difference between the OHB and OG experiments gives the impact of the NH ice sheets.

Journal Pre-proof

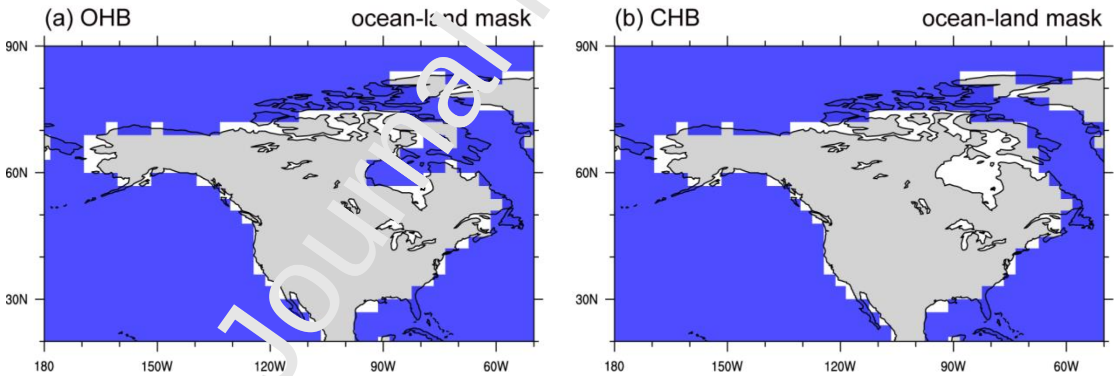

Fig. 4 The ocean-land mask over North America in the OHB (a) and CHB (b) experiments.

3. Results and discussion

3.1 The effect of Hudson Bay closure on global and regional climate

Fig. 5 shows the sea surface temperature (SST) changes at the nine dates when the Hudson Bay is closed, and they can be divided into two groups according to their different characteristics. In group one which includes seven of the nine dates, 17, 133, 340, 538, 627, 719 and 794 ka BP, the NH becomes warmer with the largest warming

Journal Pre-proof

of ~4 °C in the Labrador Sea, whereas the oceans in the Southern Hemisphere (SH) get cooler (Fig. 5). The mean SST over the eastern North Atlantic (40° N-80° N, 50° W-30° E) increases with the maximum of about ~0.59 °C at 719 ka BP, and the average warming of the seven dates is about ~0.45 °C. In group two which includes only 247 and 424 ka BP, the SST changes in the NH are very weak and even slightly opposite to the changes in group one, with a cooling of ~0.03 °C and ~0.26 °C respectively in the mean SST over the eastern North Atlantic. The changes in surface air temperature (SAT) show a similar pattern with the SST changes in both group one and group two (Fig. 6). In group one, there is a warming over most regions of the NH and a cooling in the SH. Over the Labrador Sea, the SAT increases by ~6 °C. In group two, the SAT change over the eastern North Atlantic is very weak at 247 ka BP, and there is a cooling at 424 ka BP. However, a large cooling of ~6 °C occurs over the Hudson Bay in both groups (Fig. 6), which is due to the replacement of ocean by ice-covered land over this region. On the other hand, a warming occurs over the Baffin Bay, Davis Strait and north Labrador Sea in both groups (Fig. 6), which is mainly due to the topography effect of the ice sheet over the Hudson Bay that alters the atmospheric stationary wave field.

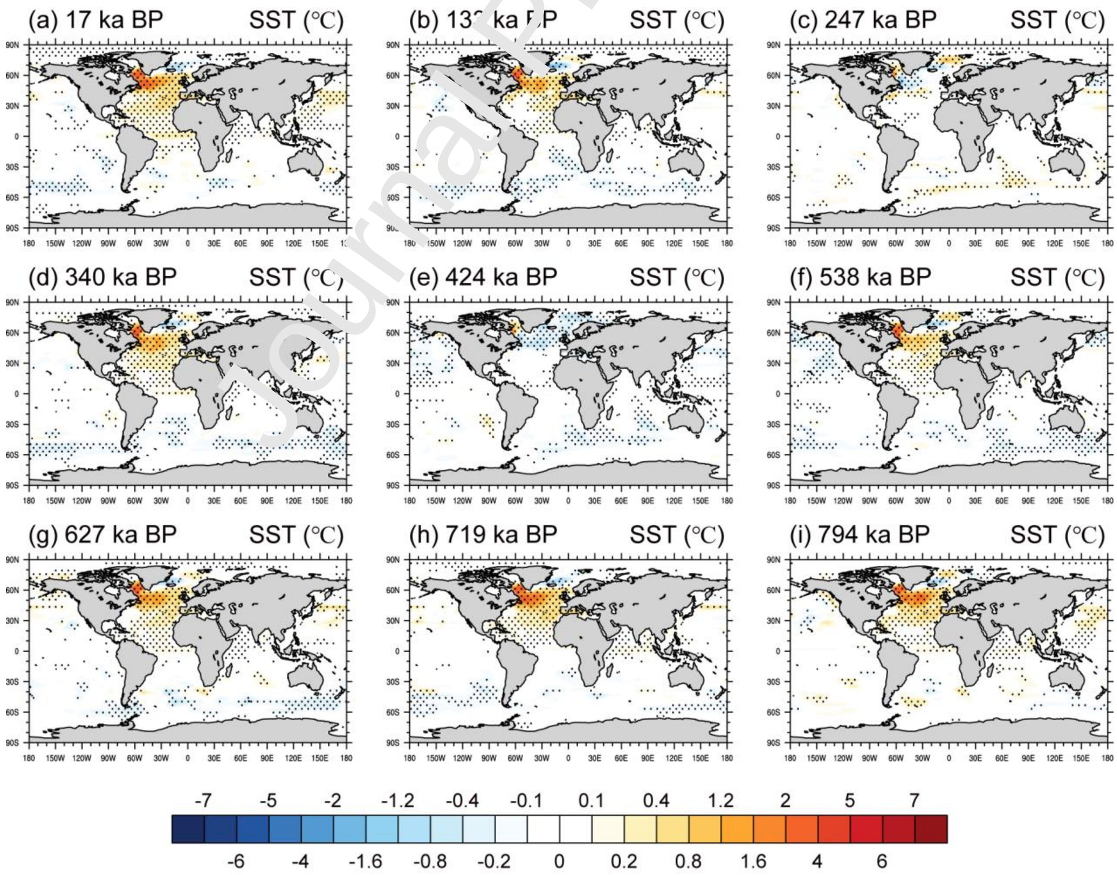

Fig. 5. Impact of the Hudson Bay closure on annual mean sea surface temperature (SST) at (a) 17 ka BP; (b) 133 ka BP; (c) 247 ka BP; (d) 340 ka BP; (e) 424 ka BP; (f) 538 ka

BP; (g) 627 ka BP; (h) 719 ka BP; (i) 794 ka BP. The difference between the CHB and OHB experiments are shown. Stippling indicates the statistically 95% significant changes by using a double sided t-test.

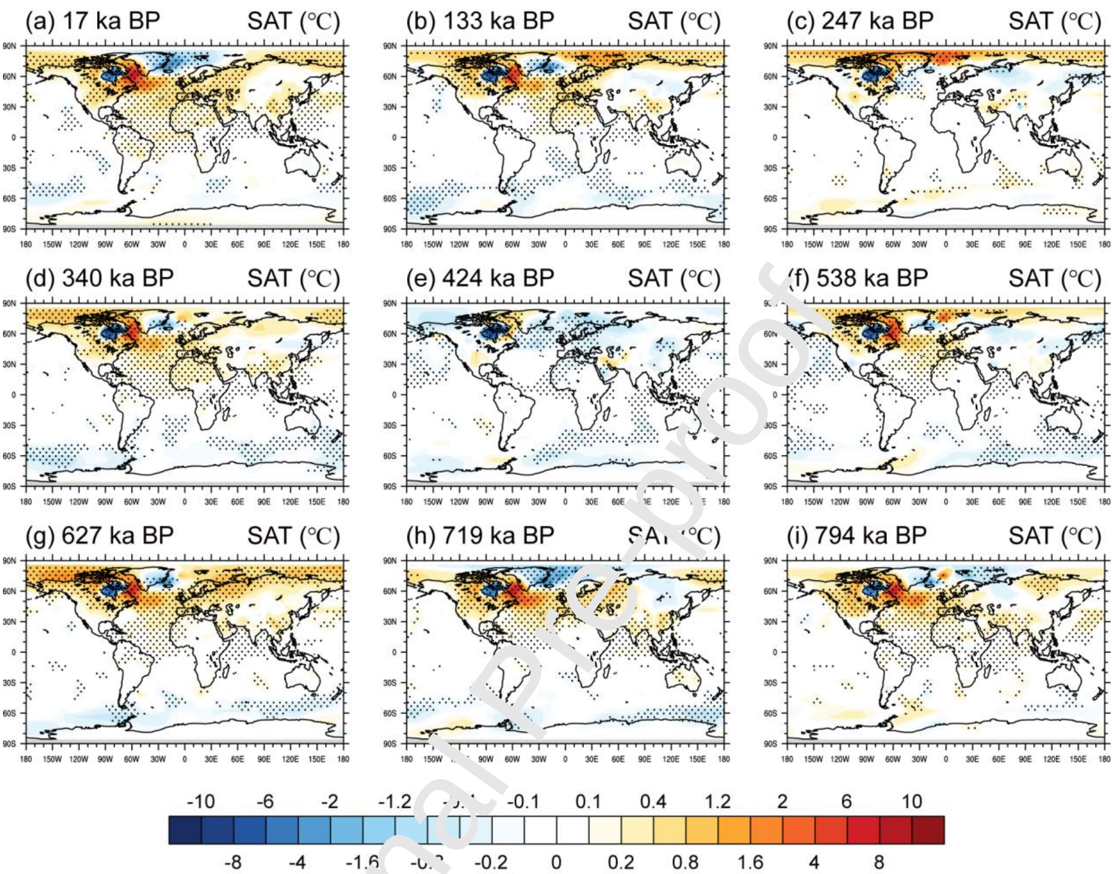

Fig. 6. Same as Fig. 5 but for annual mean surface air temperature (SAT).

In addition to temperature changes, the Hudson Bay closure also causes precipitation changes at global scale especially in the tropical regions. In group one, there is more precipitation in the tropics of the NH and less precipitation in the tropics of the SH (Fig. 7), which is related to a northward shift of the Inter-tropical Convergence Zone (ITCZ). While in group two, the variation of the ITCZ is very weak at 247 ka BP, and the ITCZ shifts southward at 424 ka BP, which leads to more precipitation in the tropics of the SH and less precipitation in the tropics of the NH (Fig. 7).

Journal Pre-proof

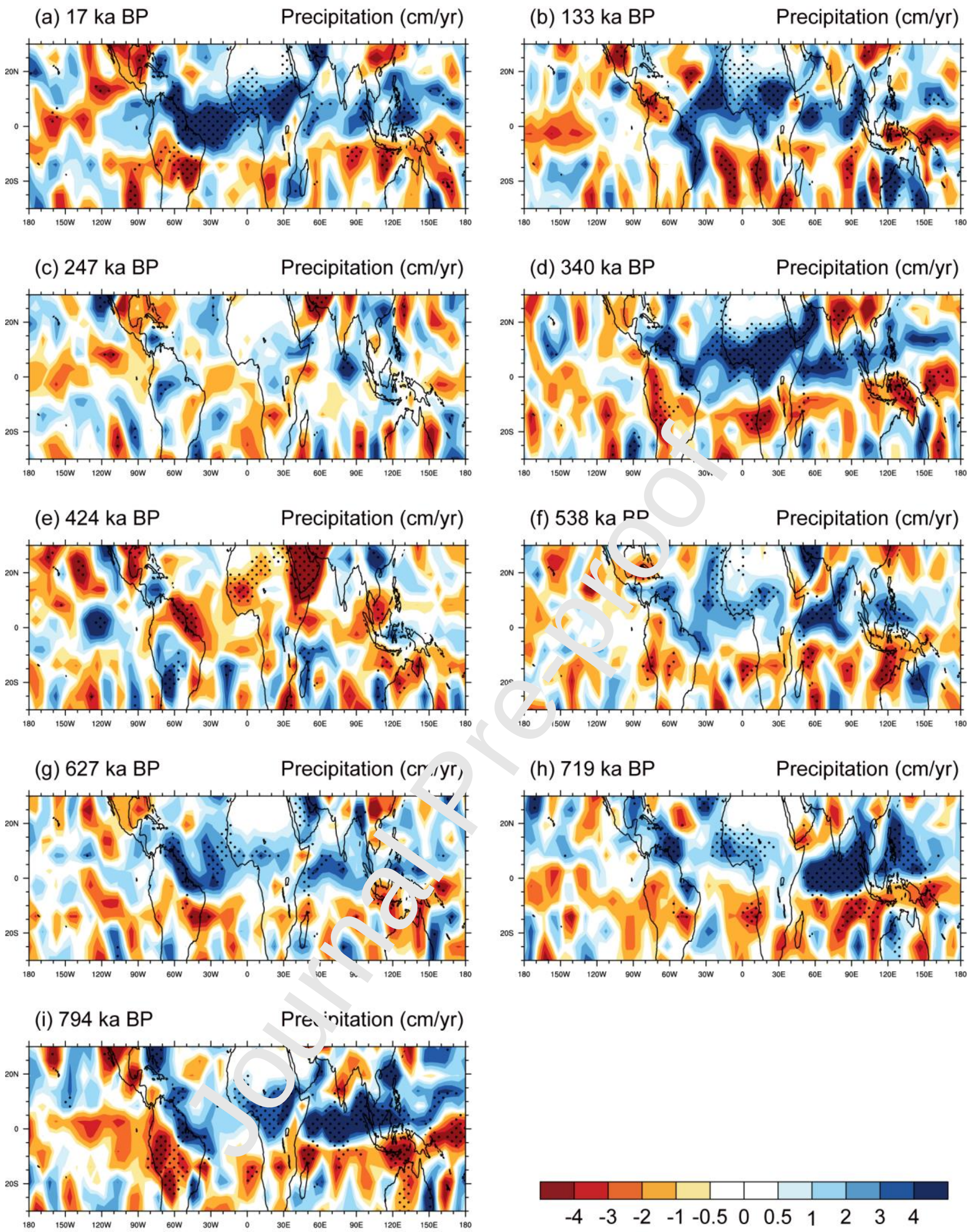

Fig. 7. Same as Fig. 5 but for annual mean tropical precipitation.

The results above show that the effect of the Hudson Bay closure could depend on background climate conditions. In group one, a warming in the NH and a cooling in the SH, and a northward shift of the ITCZ occur when the Hudson Bay is closed; while in group two, these climate changes are very weak and even slightly opposite to the changes in group one. In order to further investigate the mechanisms involved, the results of 133 ka BP and 424 ka BP are analyzed in Section 3.2 to represent group one

Journal Pre-proof

Journal Pre-proof

and group two respectively for illustration, and our additional analyses show that the processes are similar at the other dates of each group.

3.2 The forcing mechanisms for the global and regional climate changes

As mentioned above, the closure of the Hudson Bay causes a warming in the NH and a cooling in the SH, and a northward shift of the ITCZ at 133 ka BP (similar results are obtained for other dates in group one). The opposite change in temperature in the two hemispheres and a northward shift of the ITCZ are associated with a strengthening of AMOC (Fig. 8a). The increase of the AMOC strength is 8.4% at 133 ka BP, and the average increase of the seven dates in group one is 5.5%. Accompanying the strengthening of AMOC, more heat is transported into the subpolar North Atlantic from the tropical-subtropical Atlantic, leading to an increase of the northward meridional heat transport (MHT). At 40° N in the North Atlantic, the Hudson Bay closure leads to an MHT increase of 6.98% at 133 ka BP, and the average increase of the seven dates in group one is 6.22%.

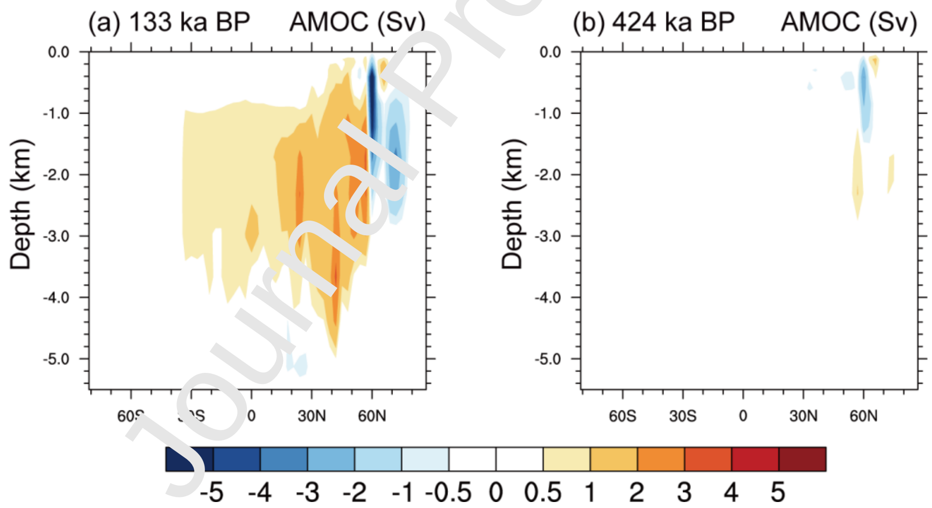

Fig. 8 Differences between the CHB and OHB experiments in Atlantic meridional streamfunction at (a) 133 ka BP and (b) 424 ka BP.

In response to the enhanced northward MHT and the large warming in the Labrador Sea (Fig. 9a and also Fig. 5, Fig. 6), sea ice substantially declines in the Labrador Sea (Fig. 9c), which would further enhance the warming. However, sea ice increases to the southeast of Greenland due to more sea ice export from the Arctic (Fig. 9c) which is driven by northeasterly wind anomaly (Fig. 9b). The increased sea ice in turn leads to a cooling to the southeast of Greenland (Fig. 9a and also Fig. 5, Fig. 6). This cooling anomaly and the one over the Hudson Bay lead to subsidence anomaly over these regions; the warming anomalies in the Labrador Sea and the northeast North Atlantic lead to ascent anomaly over these regions (Fig. 9d). These ascent and subsidence anomalies finally lead to more precipitation over both the northeast North Atlantic and the Labrador Sea but less precipitation over the Hudson Bay and southeast of Greenland (Fig. 9e).

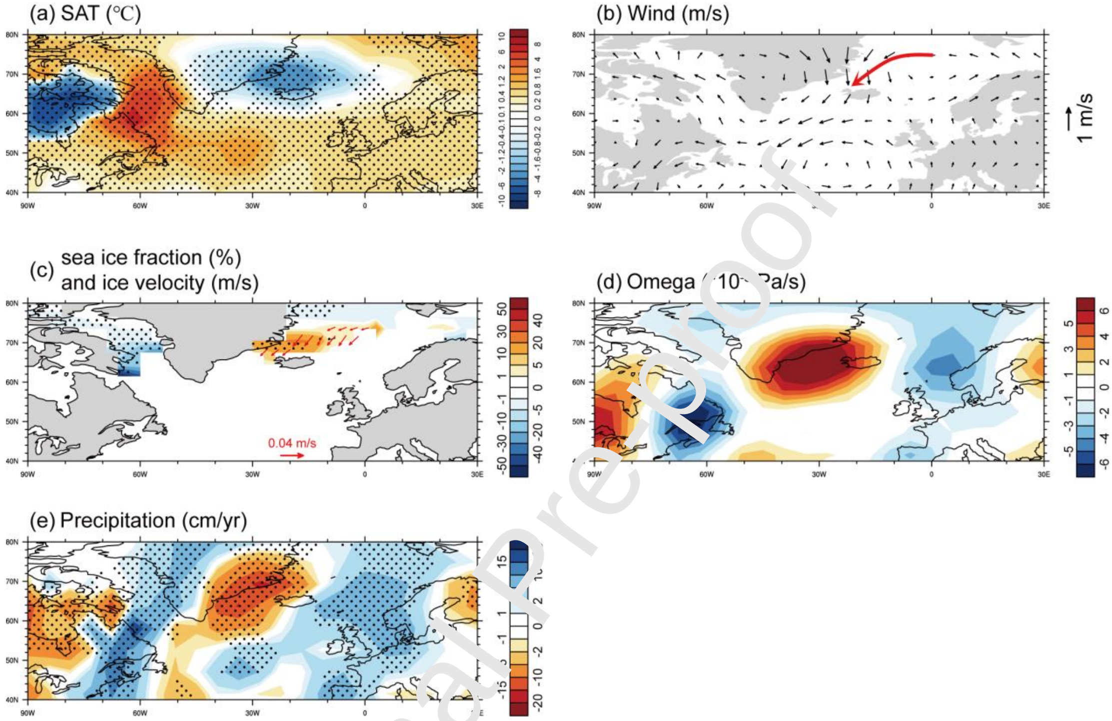

Fig. 9 Differences between the CHB and OHB experiments at 133 ka BP in: (a) SAT, (b) 800 hPa wind, (c) sea ice fraction (shaded) and ice velocity (arrows) over the sea ice increased regions, (d) 650 hPa omega field indicating vertical motion in the atmosphere (negative anomalies for ascent and positive anomalies for subsidence), and (e) precipitation. Stippling indicates the statistically 95% significant changes by using a double sided t-test.

To have a better understanding of the effect of the Hudson Bay closure at 133 ka BP, it is essential to understand how it affects the AMOC. When the Hudson Bay is closed, the evaporation minus precipitation is increased in the Labrador Sea (Fig. 10a) due to the strongly increased evaporation, which is related to the largest warming there (Fig. 9a and also Fig. 5, Fig. 6), and the sea surface water becomes saltier in the Labrador Sea (Fig. 10b), leading to denser surface water (Fig. 10c), and finally stronger

Journal Pre-proof

Journal Pre-proof

deep convection there (as diagnosed by mixed layer depth; Fig. 10d). Again, the results of other dates in group one (not show) are similar with the results at 133 ka BP. The Labrador Sea is one of major centers for deep-water formation in the North Atlantic (e.g. Thornalley et al., 2018) and also in LOVECLIM1.3 (Yin et al., 2021). The stronger deep convection in the Labrador Sea leads to a more vigorous AMOC.

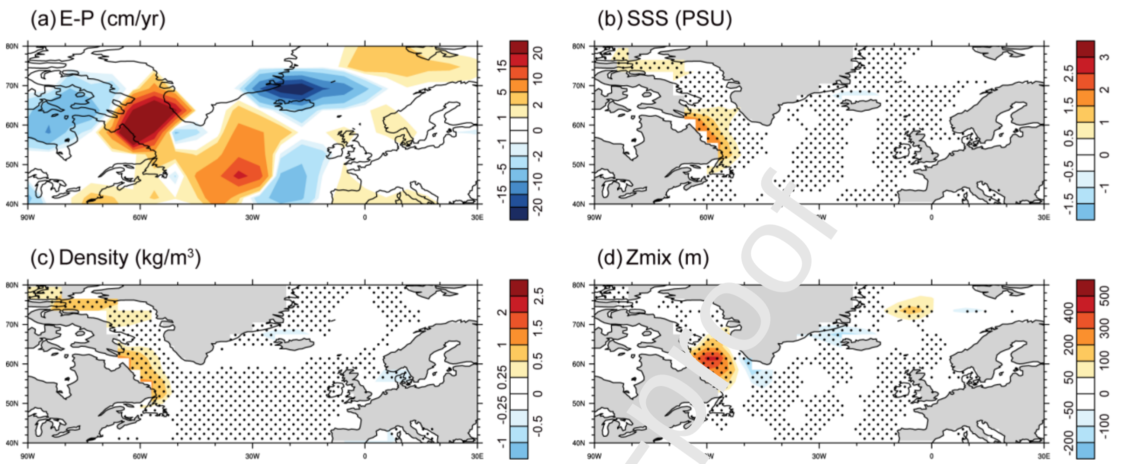

Fig. 10 Differences between the CHB and OHB experiments at 133 ka BP in (a) E - P (evaporation minus precipitation), (b) SSS, (c) sea surface density and (d) mix layer depth. Stippling indicates the statistically 95% significant changes by using a double sided t-test.

On the other hand, as mentioned above, the effect of the Hudson Bay closure at 424 ka BP is slightly opposite as compared to that at 133 ka BP, which causes a cooling in the NH and a southward shift of the ITCZ at 424 ka BP. However, both the AMOC (Fig. 9b) and the northward MHT at 40° N in the North Atlantic vary very small (less than 1%) at 424 ka BP. The cooling in the NH and a southward shift of the ITCZ at 424 ka BP should be related to the cooling over the Hudson Bay (Fig. 6) which could cool the climate locally and also in the mid-high latitudes through atmospheric circulations and sea ice feedbacks. The different effect of the Hudson Bay closure on the global and regional climate in group one and group two must be related to differences in background climate conditions. However, a simple relationship is hard to be found mainly due to the joint effect of several different forcing factors (Fig. 2 and Table 1).

3.3 Comparison of the effect of Hudson Bay closure with the effect of ice sheets

In order to assess the effect of the Hudson Bay closure in comparison with the effect of the property changes of the ice sheets themselves, we compare their respective effects on the annual mean SST and SAT using the results at 133 ka BP and 424 ka BP (Fig. 5, Fig. 6 and Fig. 11).

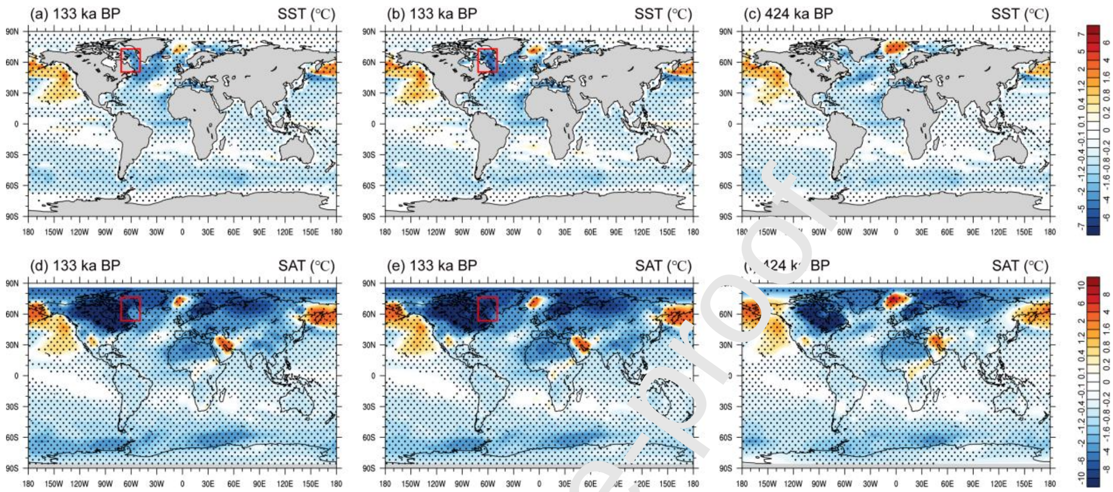

Fig. 11 The combined effect of the NH ice sheets and Hudson Bay closure on temperature at 133 ka BP, and the individual effect of the NH ice sheets on temperature at 133 ka BP and 424 ka BP. (a) SST anomaly and (d) SAT anomaly between the CHB and OG experiments, (b, c) SST anomaly and (e, f) SAT anomaly between the OHB and OG experiments. Stippling indicates the statistically 95% significant changes by using a double sided t-test.

Journal Pre-proof

As compared to the pre-industrial condition (PI), the NH ice volume increases by 23.04 and 16.52 million km^3 at 133 ka BP and 424 ka BP respectively (it is 36.93 million km^3 for the Last Glacial Maximum) (Ganopolski and Calov, 2011). The large NH ice sheets at these dates cause substantial cooling almost everywhere over the globe, especially in the high latitudes and over the ice sheets. Over the Labrador Sea, the SST decreases by ~7 °C and SAT decreases by ~10 °C at 133 ka BP (Fig. 11). The cooling in the NH at 424 ka BP is smaller than that at 133 ka BP, which is mainly due to its smaller NH ice sheets. However, there is a notable warming in the northern North Pacific in both SST and SAT. This warming has also been found in the ice sheets experiments of other studies (e.g. Yin et al., 2009; Muri et al., 2012; Ullman et al., 2014) and it is related to the topography effect of the North American ice sheet, which significantly alters the atmospheric stationary wave field and induces an increased energy-flux convergence in the northern North Pacific (e.g. Ullman et al., 2014; Liakka and Lofverstrom, 2018; Shi et al., 2020).

As compared to the effect of the NH ice sheets, the effect of the Hudson Bay closure could be quite significant, especially in the northern North Atlantic region and the surrounding continents (Fig. 5, Fig. 6 and Fig. 11). For example, at 133 ka BP, the SST increases by ~4 °C over the Labrador Sea and ~1.1 °C over the North Atlantic (40° N-80° N, 90° W-30° E) when the effect of the Hudson Bay closure is considered, while it decreases by ~7 °C over the Labrador Sea and ~2.1 °C over the North Atlantic when the effect of the NH ice sheets is considered. However, as showed in Section 3.1, the effect of the Hudson Bay closure could vary according to background climate conditions. It causes strong warming in the North Atlantic in most cases, but it could also lead to slight cooling or be very weak. Thus, in glacial climate simulations, the ice-sheet-induced cooling in the North Atlantic and a large area of the NH would be weakened (like in group one) or with no obvious change and even be slightly reinforced (like in group two) if the effect of the Hudson Bay closure is considered, depending on background climate conditions. For example, at 133 ka BP, the cooling in the Labrador Sea would be significantly decreased under the combined effect of NH ice sheets and Hudson Bay closure, as compared to the individual effect of NH ice sheets (Fig. 11).

Journal Pre-proof

4. Conclusions

In this study, the effect of Hudson Bay closure on AMOC and on global and local climate during different glacial times is investigated using the model LOVECLIM1.3. The model results show that, at 133 ka BP (other dates in group one show similar results), the Hudson Bay closure could lead to an intensification of the AMOC mainly due to the increased evaporation minus precipitation over the Labrador Sea which leads to saltier water and stronger deep convection in the Labrador Sea. The intensification of AMOC in turn leads to a warming in the NH especially in the Labrador Sea and northeast North Atlantic, a cooling in the SH, and a northward shift of the ITCZ.

However, the effect of the Hudson Bay closure on AMOC and on global climate depends to some degree on background climate conditions. For example, its effect is opposite at 424 ka BP as compared to that at 133 ka BP.

In addition to the large-scale climate changes related to the variations of AMOC, the closure of Hudson Bay also leads to notable local cooling in all the experiments. The change of the Hudson Bay from ocean to ice-covered land causes a strong cooling over the Hudson Bay region due to the modifications of surface properties and elevation. It also leads to a cooling to the southeast of Greenland due to more sea ice export from the Arctic driven by northeasterly wind anomaly.

The large-scale climate response to the NH ice sheets in our model is similar to the results obtained in other models. As compared to the effect of the NH ice sheets that existed during the studied glacial times, the effect of the Hudson Bay closure also could be very significant, especially in the northern North Atlantic and the surrounding continents. In glacial climate simulations, the ice-sheet-induced cooling in the North Atlantic and in the NH would be weakened or even be slightly enhanced if the effect of the Hudson Bay closure is considered, depending on background climate conditions.

Journal Pre-proof

Acknowledgments

This work and Z.P. Wu are supported by the Fonds de la Recherche Scientifique-FNRS (F.R.S.-FNRS) under grant MIS F.4529.18 and the National Natural Science Foundation of China (Grant No. 41888101). Q.Z. Yin is Research Associate F.R.S.-FNRS. We thank the anonymous reviewers for their constructive comments. Computational resources have been provided by the supercomputing facilities of the Université catholique de Louvain (CISM/UCL) and the Consortium des Équipements de Calcul Intensif en Fédération Wallonie Bruxelles (CÉCI) funded by the Fond de la Recherche Scientifique de Belgique (F.R.S.-FNRS) under convention 2.5020.11.

References

Berger, A., Loutre, M.F., 1991. Insolation values for the climate of the last 10 million years. Quat. Sci. Rev. 10(4), 297-317. https://doi.org/10.1016/0277-

3791(91)90033-Q

Déry, S.J., Mlynowski, T.J., Hernández-Henríquez, M.A., Straneo, F., 2011. Interannual variability and interdecadal trends in Hudson Bay streamflow. J. Mar. Syst. 88(3), 341-351. https://doi.org/10.1016/j.jmarsys.2010.12.002

dos Santos, R.A.L., Prange, M., Castañeda, I.S., Schefuß, E., Mulitza, S., Schulz, M., et al., 2010. Glacial-interglacial variability in Atlantic meridional overturning circulation and thermocline adjustments in the tropical North Atlantic. Earth Planet. Sci. Lett. 300(3-4), 407-414. https://doi.org/10.1016/j.epsl.2010.10.030

Friedrich, T., Timmermann, A., Menviel, L., Elison Timm, O., Mouchet, A., Roche, D.M., 2010. The mechanism behind internally generated centennial-to-millennial scale climate variability in an earth system model of intermediate complexity. Geosci. Model Dev. 3(2), 377-389. https://doi.org/10.5194/gmd-3-377-2010

Ganopolski, A., Calov, R., 2011. The role of orbital forcing, carbon dioxide and regolith in 100 kyr glacial cycles. Clim. Past. 7(4), 1415-1425. https://doi.org/10.5194/cp-7-1415-2011

Goosse, H., Brovkin, V., Fichefet, T., Haarsma, R., Huybrechts, P., Jongma, J., Mouchet, A., Selten, F., . Barriat, P.-Y., Campin, J.-M., Deleersnijder, E., Driesschaert, E., Goelzer, H., Janssens, I., Loutre, M.-F., Morales Maqueda, M. A., Opsteegh, T., Mathieu, P.-P., Munhoven, G., Pettersson, E.J., Renssen, H., Roche, D.M., Schaeffer, M., Tartinville, B., Timmermann, A., Weber, S. L., 2010. Description of the Earth system model of intermediate complexity LOVECLIM version 1.2. Geosci. Model Dev. 3, 603-633. https://doi.org/10.5194/gmd-3-603-2010

Liakka, J., Lofverstrom, M., 2018. Arctic warming induced by the Laurentide Ice Sheet topography. Clim. Past. 14(6), 887-900. https://doi.org/10.5194/cp-14-887-2018

Lochte, A.A., Repschläger, J., Kienast, M., Garbe-Schönberg, D., Andersen, N., Hamann, C., Schneider, R., 2019. Labrador Sea freshening at 8.5 ka BP caused by Hudson Bay Ice Saddle collapse. Nat. Commun. 10(1), 1-9. https://doi.org/10.1038/s41467-019-08408-6

Lochte, A. A., Schneider, R., Kienast, M., Repschläger, J., Blanz, T., Garbe-Schönberg, D., Andersen, N., 2020. Surface and subsurface Labrador Shelf water mass conditions during the last 6000 years. Clim. Past. 16(4), 1127-1143. https://doi.org/10.5194/cp-16-1127-2020

Loulergue, L., Schilt, A., Spahni, R., Masson-Delmotte, V., Blunier, T., Lemieux, B., Barnola, J-M., Raynaud, D., Stocker, T.F., Chappellaz, J., 2008. Orbital and millennial-scale features of atmospheric CH_4 over the past 800,000 years. Nature 453, 383-386. https://doi.org/10.1038/nature06950

Loutre, M.F., Fichefet, T., Goosse, H., Huybrechts, P., Goelzer, H., Capron, E., 2014. Factors controlling the last interglacial climate as simulated by LOVECLIM1.3. Clim. Past. 10(4), 1541-1565. https://doi.org/10.5194/cp-10-1541-2014

Luthi, D., Le Floch, M., Bereiter, B., Blunier, T., Barnola, J. M., Siegenthaler, U., Raynaud, D., Jouzel, J., Fischer, H., Kawamura, K., Stocker, T.F., 2008. High-resolution carbon dioxide concentration record 650,000–800,000 years before present. Nature 453, 379–382. https://doi.org/10.1038/nature06949

Meccia, V.L., Mikolajewicz, U., 2018. Interactive ocean bathymetry and coastlines for simulating the last deglaciation with the Max Planck Institute Earth System Model (MPI-ESM-v1. 2). Geosci. Model Dev. 11(11), 4677-4692. https://doi.org/10.5194/gmd-11-4677-2018

Muri, H., Berger, A., Yin, Q.Z., Voldoire, A., Mélia, D.S.Y., Sundaram, S., 2012. SST and ice sheet impacts on the MIS-13 climate. Clim. Dyn. 39(7), 1739-1761. https://doi.org/10.1007/s00382-011-1216-9

Kageyama, M., Albani, S., Braconnot, P., Harrison, S. P., Hopcroft, P. O., Ivanovic, R.F., Lambert, F., Marti, O., Peltier, W.R., Peterschmitt, J-Y., Roche, D.M., Tarasov, L., Zhang, X., Brady, E. C., Haywood, A.M., LeGrande, A.N., Lunt, D.J., Mahowald, N.M., Mikolajewicz, U., Nisancioglu, K.H., Otto-Bliesner, B.L., Renssen, H., Tomas, R.A., Zhang, Q., Abe-Ouchi, A., Bartlein, P.J., Cao, J., Li, Q., Lohmann, G., Ohgaito, R., Shi, X.X, Volodin, E., Yoshida, K., Zhang, X., Zheng, W.P., 2017. The PMIP4 contribution to CMIP6-Part 4: Scientific objectives and experimental design of the PMIP4-CMIP6 Last Glacial Maximum experiments and PMIP4 sensitivity experiments. Geosci. Model Dev. 10(11), 4035-4055. https://doi.org/10.5194/gmd-10-4035-2017

Journal Pre-proof

Rennermalm, A.K., Wood, E.F., Weaver, A.J., Eby, M., Déry, S.J., 2007. Relative sensitivity of the Atlantic meridional overturning circulation to river discharge into Hudson Bay and the Arctic Ocean. J. Geophys. Res.: Biogeosci. 112(G4). https://doi.org/10.1029/2006JG000330

Schilt, A., Baumgartner, M., Blunier, T., Schwander, J., Spahni, R., Fischer, H., Stocker, T.F., 2010. Glacial-interglacial and millennial-scale variations in the atmospheric nitrous oxide concentration during the last 800,000 years. *Quat. Sci. Rev.* 29(1-2), 182-192. https://doi.org/10.1016/j.quascirev.2009.03.011

Shi, F., Yin, Q.Z., Nikolova, I., Berger, A., Ramstein G., Guo, Z.T., 2020. Impacts of extremely asymmetrical polar ice sheets on the East Asian summer monson during the MIS-13 interglacial. Quat. Sci. Rev. 230, 106164, https://doi.org/10.1016/j.quascirev.2020.106164

Smith, R.S., Gregory, J., 2012. The last glacial cycle: transient simulations with an AOGCM. Clim. Dyn. 38(7), 1545-1559. https://doi.org/10.1007/s00382-011-1283-y

Straneo, F., Saucier, F., 2008. The outflow from Hudson Strait and its contribution to the Labrador Current. Deep Sea Res., Part I, 55(8): 926-946. https://doi.org/10.1016/j.dsr.2008.03.012

Tan, N., Contoux, C., Ramstein, G., Sun, Y., Dumas, C., Sepulchre, P., Guo, Z.T., 2020. Modeling a modern-like pCO_2 warm period (Marine Isotope Stage KM5c) with two versions of an Institut Pierre Simon Laplace atmosphere–ocean coupled general circulation model. Clim. Past. 16(1): 1-16. https://doi.org/10.5194/cp-16-1-2020

Thornalley, D.J., Oppo, D.W., Ortega, P., Robson, J.I., Brierley, C.M., Davis, R., Hall, I.R., Moffa-Sanchez, P., Rose, N.L., Spooner, P.T., Yashayaev, I., Keigwin, L.D., 2018. Anomalously weak Labrador Sea convection and Atlantic overturning during the past 150 years. Nature 556(7700), 227-230. https://doi.org/10.1038/s41586-018-0007-4

Ullman, D.J., LeGrande, A.N., Carlson, A.E., Anslow, F.S., Licciardi, J.M., 2014. Assessing the impact of Laurentide Ice Sheet topography on glacial climate. Clim.

Journal Pre-proof

Past. 10(2), 487-507. https://doi.org/10.5194/cp-10-487-2014

Wagner, A.J., Morrill, C., Otto-Bliesner, B.L., Rosenbloom, N., Watkins, K.R., 2013. Model support for forcing of the 8.2 ka event by meltwater from the Hudson Bay ice dome. Clim. Dyn. 41(11-12), 2855-2873. https://doi.org/10.1007/s00382-013-1706-z

Yin, Q.Z., 2013. Insolation-induced mid-Brunhes transition in Southern Ocean ventilation and deep-ocean temperature. Nature 494(7436): 222-225. https://doi.org/10.1038/nature11790

Yin, Q.Z., Berger, A., Crucifix, M., 2009. Individual and combined effects of ice sheets and precession on MIS-13 climate. Clim. Past. 5(2): 229-243. https://doi.org/10.5194/cp-5-229-2009

Yin, Q.Z., Wu, Z.P., Berger, A., Goosse, H., Hodell, D., 2021. Insolation triggered abrupt weakening of Atlantic circulation at the end of interglacials. Science 373(6558): 1035-1040. DOI: 10.1126/science.abg1737

Declaration of interests

The authors declare that they have no known competing financial interests or personal relationships that could have appeared to influence the work reported in this paper.

Highlights:

- The closure of the Hudson Bay could lead to a strengthening of the Atlantic Meridional Overturning Circulation.
- The effect of the Hudson Bay closure could be quite significant as compared to the effect of ice sheets.
- The effect of the Hudson Bay closure depends on background climate conditions.

Journal Pre-proof